72nd Highway Geology Symposium

2023 PROCEEDINGS

August 14–17, 2023 • Hotel Murano • Tacoma, Washington

Grateful Acknowledgments

We would like to thank the following people who helped make made this Symposium possible.

Samantha Denham
John Pilipchuk
Gabe Taylor
Sam Johnston
Kerri Woehler
Jon Major
Eric Smith
HGS Steering Committee
Washington Geological Survey
Pat Pringle
Delaney Event Management
Todd Hansen
Krystle Pelham

Advancing Subsurface Investigations Beyond The Borehole With Passive Seismic Horizontal-To-Vertical Spectral Ratio And Electromagnetic Geophysical Methods At Transportation Infrastructure Sites In New Hampshire

James Degnan
U.S. Geological Survey
New England Water Science Center
331 Commerce Way
Pembroke, NH 03275-3718
603-226-7826
jrdegnan@usgs.gov

Krystle Pelham
New Hampshire Dept. of Transportation
Bureau of Materials and Research
PO Box 483, 5 Hazen Drive,
Concord, NH 03302-0483
603-271-1657
Krystle.Pelham@dot.nh.gov

Neil Terry
U.S. Geological Survey
New York Water Science Center
425 Jordan Road
Troy, NY 12180
860-487-7402 Ext. 18
nterry@usgs.gov

Sydney Welch
U.S. Geological Survey
New England Water Science Center
331 Commerce Way
Pembroke, NH 03275-3718
603-226-7800
smwelch@usgs.gov

Carole Johnson
U.S. Geological Survey
Water Resources Mission Area
11 Sherman Place, Unit 5015
University of Connecticut
Storrs Mansfield, CT 06269
860-487-7402
cjohnson@usgs.gov

Prepared for the 72nd Highway Geology Symposium, August 2023

Acknowledgments

Appreciation is expressed for site access coordination and preliminary geotechnical information sharing by Chuck Corliss, NHDOT Railroad Operations Engineer and Kurt Yuengling and Adam Carr, NHDOT Geologists. Michael Howley, New Hampshire Geological Survey Geophysicist, provided data, data collection assistance, and site information. Deirdre Nash of the NHDOT Research Advisory Council provided help coordinating the project and project meetings with the technical advisory group. Jeffrey Reid of Hager Richter Geoscience offered project advice through participation in the technical advisory group and led data collection in the field with his equipment and a new method to help verify results.

Eric White of the U.S. Geological Survey Hydrologic Remote Sensing Branch, provided training to project staff in the use and interpretation of the geophysical data and assisted in the collection of field data. Tom Mack, U.S. Geological Survey Office of International Programs, provided training to project staff in the collection and processing of the geophysical data and completed a technical review of a draft of this manuscript. Colton Medler, U.S. Geological Survey Dakota Water Science Center, completed a technical review of a draft of this manuscript. Adam Benthem, U.S. Geological Survey New England Water Science Center, provided geomorphology expertise and assisted with data collection and management. Jeremy Foote, U.S. Geological Survey New England Water Science Center, provided GIS and remote sensing support. Any use of trade, firm, or product names is for descriptive purposes only and does not imply endorsement by the U.S. Government.

Disclaimer

Statements and views presented in this paper are strictly those of the author(s), and do not necessarily reflect positions held by their affiliations, the Highway Geology Symposium (HGS), or others acknowledged above. The mention of trade names for commercial products does not imply the approval or endorsement by HGS.

ABSTRACT

The U.S. Geological Survey (USGS), in cooperation with the New Hampshire Department of Transportation (NHDOT), surveyed transportation infrastructure sites using rapidly deployable geophysical methods to assess benefits added to a comprehensive site characterization with traditional geotechnical techniques. Horizontal-to-vertical spectral-ratio (HVSR) passive-seismic and electromagnetic-induction (EMI) methods were applied at four sites including a roadway-stream crossing, roadway-bridge rail-trail crossing, commuter-parking expansion, and a railroad-adjacent river-cutbank slope-failure site. Additionally, ground-penetrating radar (GPR) was used at the slope-failure site. Typically, at transportation projects, subsurface geotechnical properties are determined from boring data; however, borings are often spaced hundreds of feet apart, potentially missing important spatial variability between boreholes. Geotechnical site characterization including geophysical surveys helped provide a more accurate characterization by using continuous or near continuous profiling.

Three-component ambient noise measured with the HVSR method was used to determine site resonance frequency for estimating sediment thickness. The method works best when there is a strong shear-wave acoustic impedance contrast (> 2:1) between sediment and bedrock. Sediment thickness estimates from HVSR measurements were combined with boring data to make detailed maps of the bedrock surface elevation. The bulk electrical conductivity of the subsurface was indirectly measured with EMI methods and was used to identify lithologic variations, shallow bedrock, and conductive groundwater. Ground penetrating radar, which transmits pulses of electromagnetic energy into the subsurface and records the amplitude and timing of reflected signals, was used to identify bedding and changes in lithology or water content. By combining geophysical and boring data analyses, transportation projects produced more spatially comprehensive representations of geotechnical subsurface conditions than would be determined using conventional borings alone.

INTRODUCTION

Geotechnical site characterization guided by direct information from conventional borings, which is often used at the initiation of roadway projects by departments of transportation, sometimes cannot fully characterize the subsurface (overburden stratigraphy, hydrologic conditions, and the bedrock topography). Incompletely characterized field sites with unknown subsurface complexity between borings can disrupt work plans, force revision of designs, and lead to cost increases from schedule delays or change orders (Boeckmann and Loehr, 2016). Typically, sediment samples and water levels are obtained from the subsurface during drilling to characterize geotechnical properties, but often, due to the prohibitive expense of drilling, borings are spaced hundreds of feet apart. Additional detail from geophysical surveys could help provide a more thorough characterization of the subsurface, such as a locally shallow water table, by enabling more accurate interpolation between borings. By combining analysis of geophysical and boring data, transportation projects can produce a more comprehensive representation of geotechnical subsurface conditions than can be determined using conventionally spaced borings alone.

Incorporation of more geophysical measurements into transportation projects is recognized by goals established in the Federal Highway Administrations EDC-5: Advanced

Geotechnical Methods in Exploration (A-GaME) initiative (U.S. Department of Transportation, Federal Highway Administration, 2020). Data collection in support of these goals could help assess the utility of such methods in improving geotechnical characterization at New Hampshire Department of Transportation (NHDOT) roadway project sites. Results can be used to evaluate the potential to improve timing of project completion and cost savings. Geophysical data collected using methods such as HVSR and EMI at sites in New Hampshire (fig. 1) could help identify geologic and hydrologic conditions that can affect transportation infrastructure planning, design, construction, and maintenance. A variety of NHDOT infrastructure sites requiring geotechnical investigations planned in 2022 were selected by this project for HVSR and EMI geophysical data collection and analysis. Geotechnical properties of the subsurface from boring data from previous and ongoing investigations, as well as other information from geologic maps, landfill feasibility hydrogeological investigations, and remote sensing can be considered to constrain geophysical investigation interpretations.

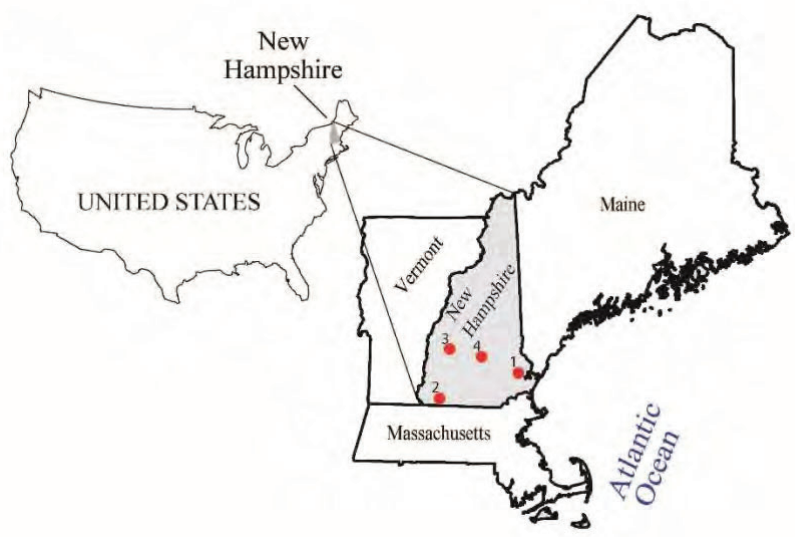

Figure 1. Map showing site numbers and locations (red circles): site 1: roadway crossing stream, Lee, New Hampshire; site 2: roadway crossing rail trail, Troy, New Hampshire; site 3: carpool and bus stop parking, New London, New Hampshire; and site 4: railroad adjacent to slope failure, Canterbury, New Hampshire.

The purpose of this study is to assess the utility of integrating geophysical techniques with routine geotechnical assessments to provide additional information to ongoing NHDOT projects in varied transportation infrastructure, geotechnical, and hydrogeologic settings. Results from this study can also be used to guide future survey designs and to further refine geophysical results at future NHDOT and USGS investigation sites.

Methods of data collection and analysis

Two primary geophysical methods were used in the study: (1) passive horizontal-to-vertical spectral ratio (HVSR) seismic (Cox and others, 2020; Johnson and Lane, 2016; Mack, 2020) and (2) frequency domain electromagnetic induction (EMI) (Huang and Won, 2000). Ground penetrating radar (GPR) was also used at one site where additional characterization was needed. These methods were chosen because they can be rapidly deployed and are well suited for

improving cross sections of the subsurface compared to those generated with conventionally spaced borings alone.

Analysis focused on improvement in bedrock-surface, stratigraphic, and saturated-zone mapping for geotechnical site characterization. Regional and local surface-water and groundwater quality, geologic, and hydrologic data were reviewed to help site characterization and to categorize method efficacy in a variety of typical NHDOT settings. Enhanced cross sections of subsurface conditions can then be generated with integrated results of borings (Yuengling, K. R., 2022, Carr, A. R., 2022a and b, and Jacques Whitford Company, Inc., 2004) and geophysical surveys to improve site characterization.

HVSR is not widely used but the effectiveness of the methods of data processing and associated regression models have been documented regionally and by specific site. The method requires developing accurate regression models with coefficients that are representative of the region or site where the data are collected. For example, the development of a data base of regression coefficients determined for specific materials at sites or within regions could help NHDOT and others streamline future HVSR seismic processing. Electromagnetic induction and GPR methods provide independent information based on unique responses to electrical properties of the subsurface; EMI measures electrical apparent conductivity (average of a given half space), whereas GPR measures distinct boundaries of materials with different properties with patterns that often give an indication of general sediment grainsize (Beres and Haeni, 1991; Haeni, 1996). However, sites where the subsurface and groundwater electrical conductivity might be altered by road salt may limit the utility of some geophysical methods such as EMI and GPR due to attenuation of the signal; alternatively at some sites, such conditions might enhance the utility of geophysical methods. It is important to consider geologic information and hydrologic data to understand how seasonal or hydrologic event-based conditions (drought or flooding) might affect data interpretation.

Horizontal-to-vertical spectral ratio

The HVSR method is used to determine the peak resonance frequency (f_0) induced by ambient seismic noise in unconsolidated sediments overlying bedrock when there is an adequate contrast in shear-wave acoustic impedance between the two layers (> 2:1). Spectral ratio analysis of the combined horizontal and vertical components of the seismic data was used to determine f_0. A regression model (equation) to solve for sediment thickness using a power law function fit to the HVSR-determined f_0 versus depth to rock was developed to use in HVSR seismic data processing equations (Bignardi, 2017, Johnson and Lane, 2016, Mack, 2020, and Medler, 2021). Plots of the horizontal to vertical spectral ratio versus resonance frequency were examined to determine a qualitative peak frequency quality. The peak frequency quality is a qualitative classification, on a scale from 1 to 5, and is based on how clear and sharp the peak is with 5 being the best and 1 being the worst. The quality of the HVSR result peak and the maximum horizontal to vertical spectral ratio standard deviation generated by the processing software (MOHO, 2020, SESAME WP04, 2004) were compared to data collection conditions. Three HVSR seismometers were deployed simultaneously at different measurement locations at each site to maximize data collection time efficiency. A variety of coupling techniques were tested in different settings, as seismometer coupling to the ground affects data quality. Additional information about the surveys and data are available in a data release (Degnan and others, 2022).

Shear wave velocities (v_s) were computed for each HVSR measurement with an adjacent boring with a known depth to bedrock using equation 1. Mean shear wave velocities for each site were used to calculate bedrock depth from HVSR measurements that were not near borings for bedrock surface profiling and mapping using equation 2 (Johnson and Lane, 2016).

$$v_s = z\,(f_0 * 4); \quad (1)$$

$$z = v_s/(f_0 * 4) \text{ and} \quad (2)$$

where

z is the depth to bedrock in feet;
v_s is the overburden shear wave velocity in feet per second; and
f_0 maximum (peak) horizontal to vertical spectral ratio in Hertz.

Electromagnetic induction

Bulk electrical conductivity of the subsurface was indirectly measured with EMI methods using induced electromagnetic fields (Zohdy and others, 1974) at several frequencies and coil spacings. Frequencies with sufficient signal to noise ratio for a given survey were selected for inverse modeling to better understand conductivity variations with depth (Abraham and others, 2006). Variations in electrical conductivity, both laterally and vertically, were measured with one of two frequency-domain EMI instruments used in this study: (1) multiple frequency GEM-2 and (2) the larger, multiple spacing and dual orientation, DUALEM-421. The GEM-2 has a fixed transmitter-receiver (Tx-Rx) coil spacing and sweeps through several logarithmically-separated transmitter frequencies. Measurements made with lower frequencies are generally capable of sensing deeper apparent conductivity values at the cost of a lower signal to noise ratio, while measurements made with higher-frequencies provide shallower but increased signal to noise ratio. The DUALEM-421 uses a single 9-kHz frequency with multiple Tx-Rx coil spacings and orientations, where measurements made with larger coil spacings sense a larger volume and hence deeper conductivity values, while shorter coil spacings provide increased resolution of the shallow subsurface. Additional information about the surveys, data, and processing are available in a data release (Welch and others, 2023).

Raw data from the GEM-2 consist of measurements of the real and imaginary normalized magnitude of the magnetic field quadrature at each of the transmitter frequencies (in units of parts per million). A further processing step can be applied to convert these values to apparent electrical conductivity and apparent magnetic susceptibility using the Invertor software (Geophex). This analytic conversion assumes an electromagnetically homogeneous earth below the sensor. The DUALEM-421 automatically performs the conversion from normalized magnetic field components to apparent electrical conductivity and magnetic susceptibility.

Data were processed to remove erroneous data points that were characterized by extreme high or low values (noise) following the methods described by Johnson and others (2019) and resampled to 1-meter spacing using a moving averaging window. The apparent conductivity data were inverted with a Laterally Constrained Inversion to produce depth versus electrical resistivity (1/conductivity) along 2D profiles. This type of inversion encourages a smoothed out but stable solution when fitting data to models. As part of the inversion process, a depth of investigation (DOI) was computed to estimate the depth to which the measurement is reliable (Christiansen and Auken, 2012). Results were output as text files that included positions, DOI, inversion metrics (data and model residual), and inverted resistivity models (Welch and others, 2023);

these outputs were used to generate profiles of electrical conductivity to compare to other data using plotting tools in R (R Core Team, 2023; Wickham, 2016).

Ground-penetrating radar

Ground-penetrating radar (GPR) profiles were generated with an antenna with a fixed Tx-Rx offset contained within a tow-body. GPR transmits pulses of electromagnetic energy into the subsurface and records the amplitude and timing for the return of reflected signals to image the subsurface (Keary and Brooks, 1991). The radar-wave propagation is affected by electromagnetic properties of the subsurface materials including dielectric permittivity, electrical conductivity, and magnetic susceptibility caused by differences in lithology, water content and specific conductance, and sediment type (Milsom, J. and Eriksen, A. 2011). The penetration of GPR signals is limited where bulk electrical conductivity of the subsurface is high or where the radar-wave reflection is scattered from discrete objects too small to generate a coherent geometric reflection, such as large cobbles. Here, GPR data were collected using an 80-MHz shielded antenna. Depth to reflectors is not inherently known from GPR data, given that the speed at which radar waves travel depends on study area subsurface properties. Therefore, estimates of GPR velocity are required to present GPR data with a depth axis to estimate depths to observed reflectors. Published velocity estimates (Beres and Haeni, 1991) and velocity measurements from diffraction hyperbola fitting in the ReflexW software (MALA, 2022) were used to calculate depth from reflected radar-wave travel time. GPR velocities used (n = 37) ranged from 0.057 meters per nanosecond to 0.22 meters per nanosecond, with a median value of 0.12 meters per nanosecond. These two end-member velocities likely represent fully saturated soils with high water content (low velocity) versus loose dry soil with significant air space (high velocity).

RESULTS

Results of HVSR, EMI, and GPR field data collection and analysis at four selected transportation infrastructure sites are presented in this section. Before discussing results from each site individually, general observations from HVSR and EMI surveys are discussed to provide background information necessary for interpretation of geophysical datasets. All data from geophysical surveys are publicly available in published data releases. Data from HVSR measurements are available in Degnan and others (2022) and EMI and GPR survey data are available in Welch and others (2023).

General geophysical surveys

One important observation from HVSR measurements was that data quality varied with distance from roadways. Frequency peaks in the best quality category (category 5) from HVSR analysis were obtained at various distances from roadways; however, the best quality category had the highest median distance from roadways (fig. 2A). Therefore, although it is possible to get good quality data near a road, most of the best-quality category data were obtained farther from roadways. Additionally, standard deviations were much smaller for measurements made 200 ft (feet) or farther from a roadway (fig. 2B). Also, the best quality data (with the lowest standard deviation) were acquired when the seismometers were well coupled in compact sands, and the highest median standard deviations were associated with loose soil, which generally has poor coupling (fig. 2C).

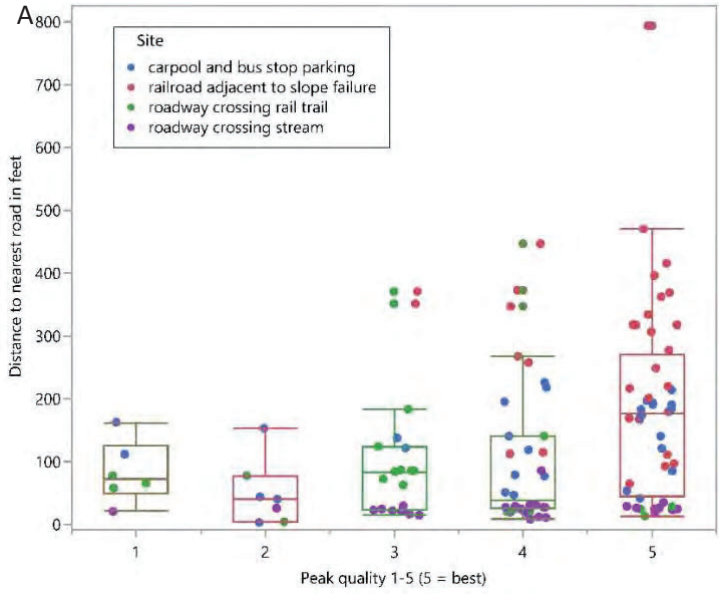
A
Site
carpool and bus stop parking
railroad adjacent to slope failure
roadway crossing rail trail
roadway crossing stream
Distance to nearest road in feet
0
100
200
300
400
500
600
700
800
1
2
3
4
5
Peak quality 1-5 (5 = best)

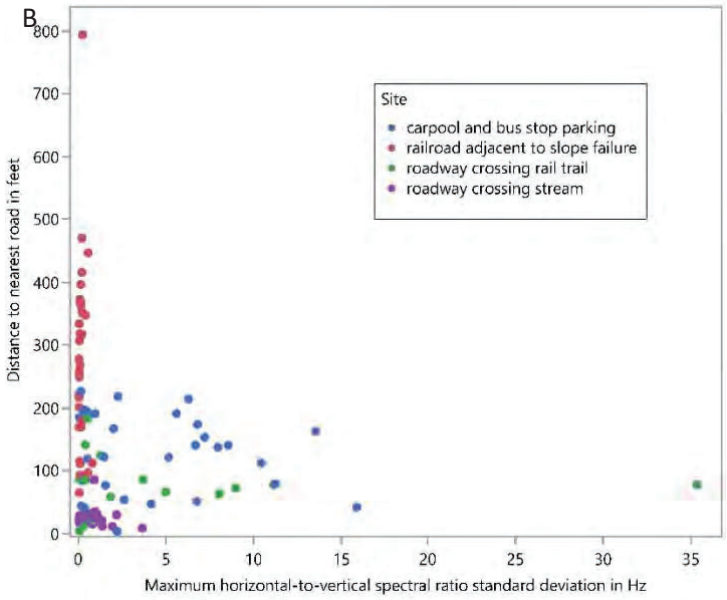
B
Site
carpool and bus stop parking
railroad adjacent to slope failure
roadway crossing rail trail
roadway crossing stream
Distance to nearest road in feet
0
100
200
300
400
500
600
700
800
0
5
10
15
20
25
30
35
Maximum horizontal-to-vertical spectral ratio standard deviation in Hz

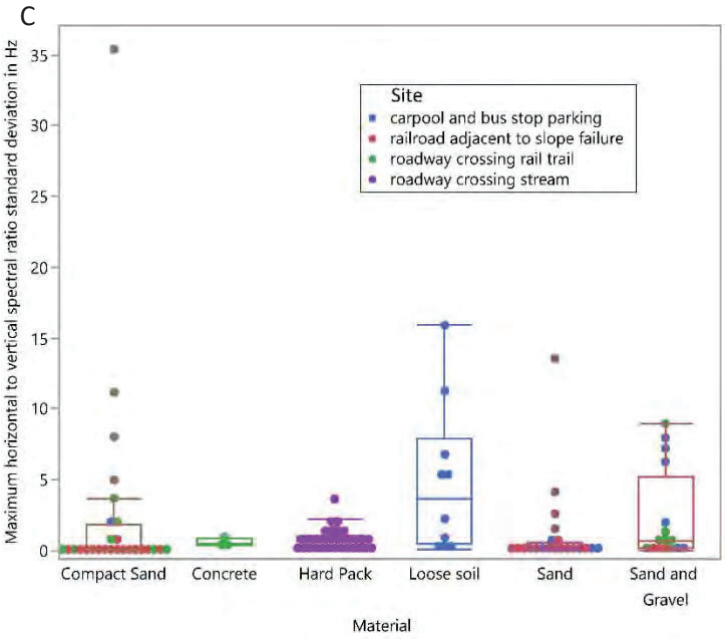

Figure 2. Charts showing passive seismic horizontal-to-vertical spectral ratio (HVSR) data quality indicators, (A) resonance frequency peak quality using a categorical rating system from 1 (worst) to 5 (best), and (B) standard deviation from horizontal-to-vertical spectral ratio measurement versus distance from nearest roadway and (C) coupling material verses horizontal-to-vertical spectral ratio measurement standard deviation.

Shear wave velocities were computed for each HVSR measurement with an adjacent boring with a known depth to bedrock (**Table 1**) using equation 1 above. Velocities were similar to those reported in other locations with similar overburden stratigraphy in the region (Marvinney and Glover, 2015). A mean site shear wave velocity was used to calculate depth to bedrock at sites with more than one boring available.

A regression equation (3) was developed using f_0 measurements and depths to bedrock from borings (Table 1) so bedrock depth can be calculated at similar sites without boring information (Lane and others, 2008).

$$z = af_0^b \text{ and} \quad (3)$$

where

z is the depth to bedrock in feet;
a computed regression parameter is 423.51;
b computed regression parameter is -1.167;
f_0 and is the resonance frequency.

The resulting regression equation, based on the 17 depths to bedrock and corresponding f_0, was similar to those generated by studies in similar nearby settings (Johnson and Lane, 2016, Fairchild and others, 2013, and Panthi and others, 2023).

Table 1. Depth to bedrock from borings and shear-wave velocities computed from maximum horizontal-to-vertical spectral ratio by site and material. [ft, feet; v_S, shear wave velocity; ft/s, feet per second; f_0, resonance frequency peak; hertz, Hz]

Site	Boring	Bedrock depth from boring, in ft	Shear-wave velocity (v_S) (ft/s)	Maximum f_0 Hz	F_0 standard deviation in Hz	Mean site v_S (ft/s)	Overburden lithologic summary
roadway crossing stream	B01	50.9	1198	5.91	1.3	1148	fill, alluvium, marine, and till
	B02	45.6	1027	5.63	0.3		fill, alluvium, marine, and till
	B03	25.3	1096	8.06	0.1		fill, alluvium, and till
	B04	36.5	1263	8.66	0.29		fill, alluvium, and till
roadway crossing rail trail	B03	92.0	1611	4.38	0.73	1628	glacial outwash and lacustrine
	B02	99.5	1656	4.16	0.37		glacial outwash and some lacustrine
	B01	102	1530	3.75	0.46		glacial outwash and some lacustrine
	B04	94.0	1715	4.56	0.82		glacial outwash, lacustrine, and some till
carpool and bus stop parking	B-08	15.1	879	14.6	1.54	984	fill and till
	B-04	14.8	1322	22.3	2.21		till
	B-06	14.4	722	12.4	0.04		fill and till
	B-02	8.86	912	25.3	0.61		glacial outwash and till
	B07	20.8	1014	12.2	0.10		fill and till
	B11	5.50	767	34.9	6.80		silt and till
	B13	5.00	399*	19.9	0.48		silt and till
	B10	7.50	1219	40.6	11.3		silt and till
	B03	7.70	1034	33.6	0.35		glacial outwash and till
railroad adjacent to slope failure	TW-103	179	1211	1.77	0.03	1211	stream terrace, glacial lake, some till

*outlier not used in mean calculation

Median apparent electrical conductivity values were similar at the four sites surveyed. The roadway crossing stream site was selected to be surveyed with both the multiple-coil spacing and multiple-frequency instruments to provide a comparison of results between the two methods. This was done because the site had several forms of interference described in the section below and had a range of overburden materials and depths. Three sites were surveyed using the multiple coil spacing instrument and two were surveyed using the multiple-frequency instrument (Table 2). The carpool and bus stop parking site had the thinnest overburden, which was mostly till that would be expected to produce a less conductive response than thick marine and lacustrine sedimentary lithologies found at the other three sites. However, the maximum values were highest at sites directly adjacent to roadways and were likely related to metal infrastructure or legacy de-icing chemicals (road salt) in groundwater (**Table 2**).

Table 2. Apparent conductivity summary statistics in millisiemens per meter (mS/m) from the electromagnetic induction surveys by site.

Site	N Rows	Mean depth of Investigation (DOI, feet)	Apparent Conductivity in mS/m				
			Mean	Median	Max	Interquartile Range	25th Percentile
roadway crossing rail trail*	2877	12.59	13.50	7.6	424.8	10.4	3.6
roadway crossing stream*	2230	18.39	8.35	7.1	215.3	7.4	3.7
roadway crossing stream**	13413	14.92	18.02	7.50	8608	7.28	3.96
railroad adjacent to slope failure*	2786	19.53	5.99	3.8	102.5	3.7	2.2
carpool and bus stop parking expansion site**	32609	10.91	28.31	7.14	31065	11.75	3.18

*Data collected with multiple-coil-spacing instrument

**Data collected with multiple-frequency instrument

SITE-SPECIFIC SURVEYS

Roadway crossing stream, site 1, Lee, New Hampshire

The roadway crossing stream site (site 1) is in Lee, NH, where the Little River flows under State Route 125 through a large metal culvert. Geotechnical investigations to support a culvert replacement design and work plan were scoped to determine the overburden stratigraphy, the depth to bedrock, existing fill materials, and the location of former bridge abutments buried on each side of the culvert beneath the roadway.

Twenty-five HVSR measurements were made at 20 measurement locations along the roadway shoulder behind the guard rail at the roadway crossing stream site. Three of the HVSR locations were selected to correspond with boring locations with documented overburden stratigraphy and depth to bedrock. The other 17 measurements were used to delineate the bedrock surface profile line within and beyond the boring investigation locations. Measurements were repeated at four locations to compare results from different traffic patterns at about 5, 10, and 15 ft from the general path of traffic. The first round of measurements was completed when the drill rig and traffic diverting package (traffic control flags, cones, and impact absorbing vehicle) were on site. Traffic diversion caused measurements on the same side of the roadway (east) as the drill rig to be about 5 ft farther from the path of vehicle travel and measurements on the opposite side of the roadway (west) were about 5 ft closer to the path of vehicle travel. In general, HVSR peak quality was better with increasing distance from the path of traffic.

The apparent conductivity results show anomalies (patterned variation) interpreted to represent the surface of the bedrock (fig. 3 A-D). Some anthropogenic effects from power lines and buried metal structures are likely present. Above-ground powerlines are located along State Route 125 and may have impacted the multiple-frequency EMI instrument dataset. Data were collected on the side of road away from the powerlines to attempt to reduce those effects.

The Little River culvert appears in multiple-frequency EMI instrument results as a broad conductive anomaly and a large in-phase anomaly. Both instruments detected a highly resistive anomaly in the middle of the surveyed area along the northwest edge adjacent to bedrock outcrop. The area of this resistive anomaly represents the expression of shallow bedrock subcropping (fig. 3A and B).

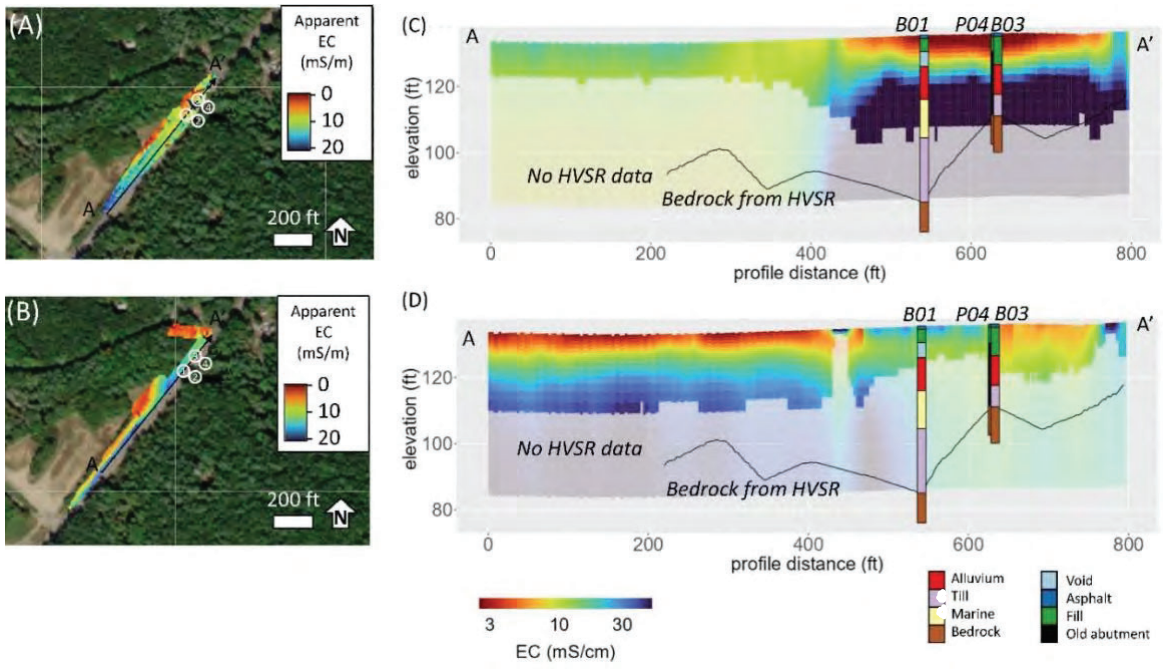

Figure 3. Electromagnetic induction survey results from the A-A' cross section at site 1, roadway crossing stream, in Lee, New Hampshire, showing (A) a map of apparent electrical conductivity (EC) from the multiple-frequency instrument 47,970 Hz band; (B) a map of apparent conductivity from the multiple-coil-spacing instrument (4-m-spaced horizontal coplanar coils); (C) profiles of inverted electrical conductivity from the multiple-frequency instrument with borings and the bedrock surface from passive seismic horizontal-to-vertical spectral ratio results; and (D) profiles of inverted electrical conductivity from the multiple-coil-spacing instrument with borings and the bedrock surface from passive seismic horizontal-to-vertical spectral ratio results. White circles with labels on panels (A) and (B) correspond to borings on panels (C) and (D).

Roadway crossing rail trail, site 2, Troy, New Hampshire

The roadway crossing rail trail site (site 2) is located in Troy, NH, where State Route 12 crosses the Cheshire Rail Trail. The rail trail is a recreational and commuter trail along a former railroad with tracks removed or buried to facilitate travel by foot or bicycle. Bedrock outcrop and blasted railroad rockcut features are aligned with the direction of the trail south of the bridge on the northwest side of the trail. Geotechnical investigations support a bridge replacement design and were scoped to characterize overburden stratigraphy, depth to bedrock, the top 10 ft

of bedrock with core, existing fill materials, and identify the extent of the existing bridge abutment footings. Despite the interference, the data shown is useful and provides information about the subsurface as described below.

Twenty-one HVSR measurements were made at 21 selected locations at the roadway crossing rail trail site; three correspond with boring locations with a documented overburden stratigraphy and depth to bedrock; and 16 measurements along the rail trail were of good quality and used to delineate the bedrock surface profile line within and beyond the boring investigation locations (fig. 4). One measurement was not used due to the lack of a clearly define peak. Measurement locations had a 65.6 ft spacing along the rail trail starting in the southwest adjacent to the railroad rockcut and extending northeast 730 ft to the bridge and 285 ft to the northeast beyond the bridge. The five measurements made adjacent to the railroad rockcut have directional H/V maximum intensities between 100- and 125-degree azimuths with a 113-degree median; whereas the deeper bedrock surface identified at the other end of the survey line north of the bridge had between 158- and 180-degree azimuth with a 170-degree median.

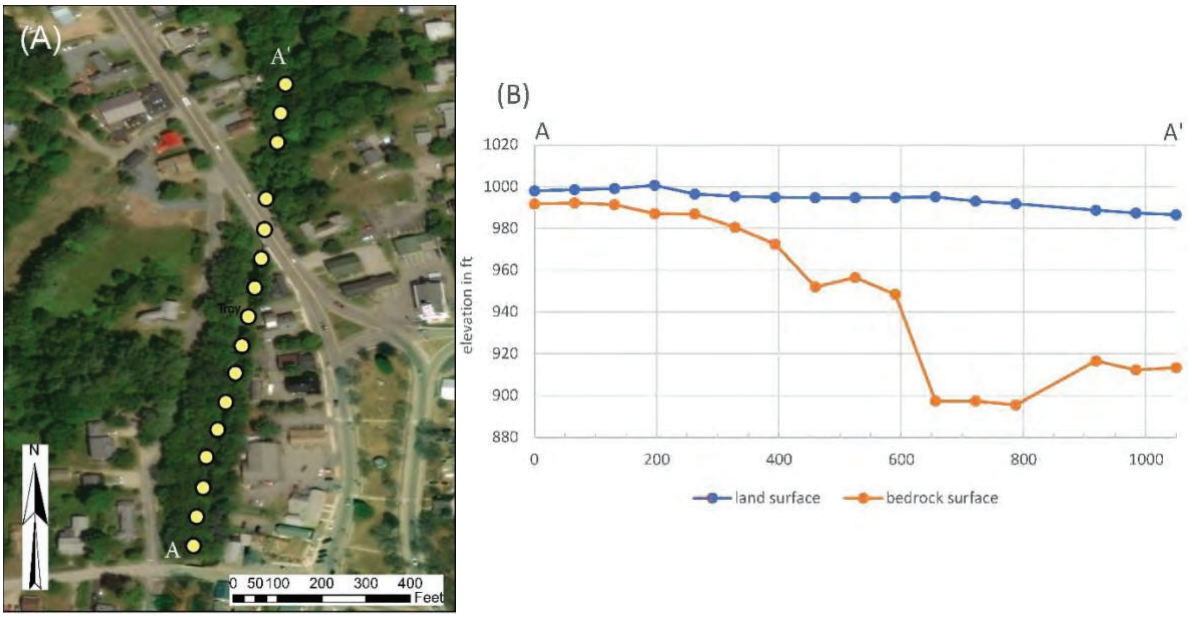

Figure 4. Passive seismic horizontal-to-vertical spectral ratio measurement results from the A-A' cross section at site 2, roadway crossing rail trail, Troy, New Hampshire, showing (A) a map of measurement locations and (B) a cross section of bedrock surface and land surface.

The EMI results from the roadway crossing rail trail site had the highest residuals and the least successful inversion of all the sites (fig. 5). This may be a result of (1) noise and (or) coupling effects which were strong and likely affected the data near shallow buried metal from the former railroad throughout the survey area and (2) metal from the State Route 12 bridge in the center of the survey area. It is possible that the old rails or other metal hardware were not removed and instead buried on site. Comparison to borings was difficult because electrical noise was higher in this area than at other sites. Inversions were successful but had higher data residuals compared to other sites. The geophysical inversion process used to analyze EMI data assumes a smoothly varying or layered bulk electrical conductivity distribution of the subsurface and has difficulty fitting features that violate these assumptions, such as discrete human-made objects.

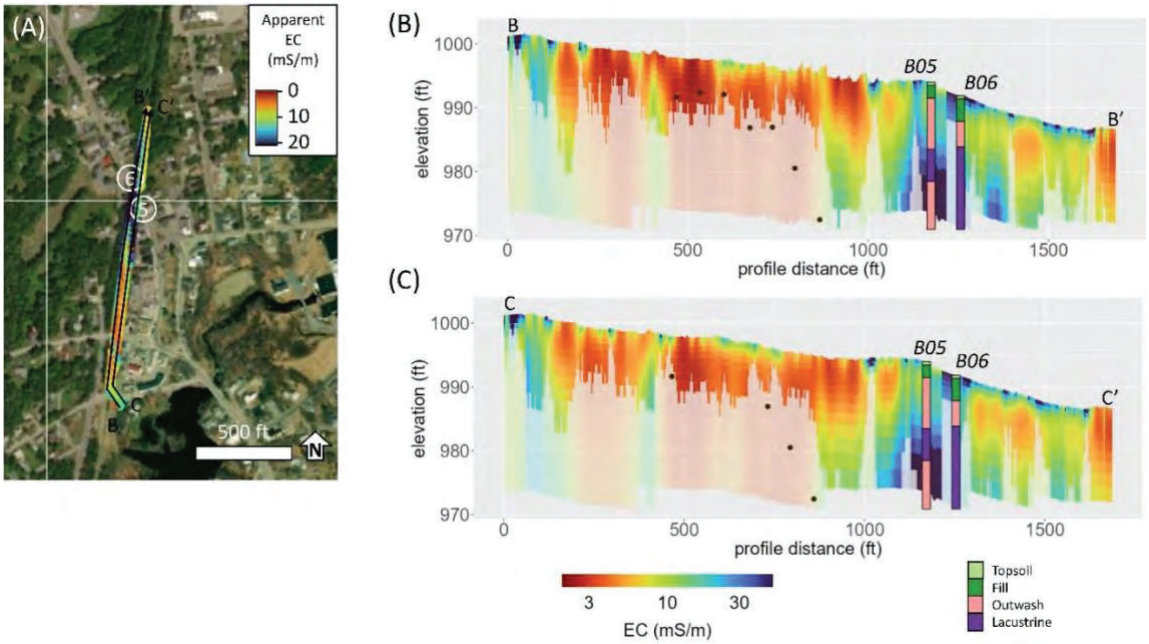

Figure 5. Electromagnetic induction survey results from the multiple-coil spacing instrument from the B-B' and C-C' cross sections at site 2, roadway crossing rail trail in Troy, NH, showing (A) a map of apparent electrical conductivity from the 4-m-spaced horizontal coplanar coils with cross section and boring locations shown with white circles and (B) and (C) profiles of electrical conductivity from inverted frequency domain electromagnetic induction data demarcated in (A). Black dots on profiles show estimated depth to bedrock from passive seismic horizontal-to-vertical spectral ratio measurements.

The bedrock surface generated with HVSR results and borings indicates shallow bedrock to the south and deep bedrock to the north (fig. 4). This is consistent with outcrops and railroad rockcuts observed at the site and with the resistive EMI results.

In general, the site results suggest a thin conductive layer overlying resistive materials. Potentially, the conductive upper layer is related to the old railroad, and the resistive materials are outwash with moisture in the vadose zone and groundwater at depth. In the area around the State Route 12 bridge and other roadways, the results indicate higher conductivity, likely due to increased porewater conductivity due to residual road salt used for deicing. Many of the shallow conductive "anomalies" visible in this profile may be related to infrastructure as opposed to soils or geology.

Carpool and bus stop parking, site 3, New London, New Hampshire

The carpool and bus stop parking site (site 3) is accessed from State Route 103A and is located between State Route 103A to the west and State Route 11 to the north and Interstate Highway 89 to the east in New London, NH. Seeps with iron fouling at the southern toe of the existing parking lot embankment drain to an unnamed stream that flows south along the west edge of the site. Geotechnical site characterization described fill materials, overburden stratigraphy, depth to bedrock, and core from the top 10 ft of bedrock in order to aid in the design of a construction plan for the extension of the parking lot.

Thirty-one HVSR measurements were made at 29 measurement locations along the parking lot shoulder, embankment, slope toe, and in the adjacent woods at the carpool and bus stop parking expansion site. Nine of the HVSR locations were selected to correspond with boring

locations with a documented overburden stratigraphy and depth to bedrock. The other 21 measurements were used to delineate the bedrock surface within and beyond boring locations. Measurements were repeated at two locations to compare results with different ground coupling methods. Two repeat measurements were completed using a gravimeter plate and had higher quality peaks and coupling signals than those collected with direct coupling. The gravimeter plate also was used at 14 other measurement locations because cobbles and tree roots prohibited direct ground coupling.

Electromagnetic induction data were collected with the multiple-frequency instrument at this site and exhibited lateral variation in apparent conductivity, but the method had limited ability to achieve the depth of investigation produced at other sites. Shallow electrically resistive bedrock may have limited the propagation of the EMI signal at this site.

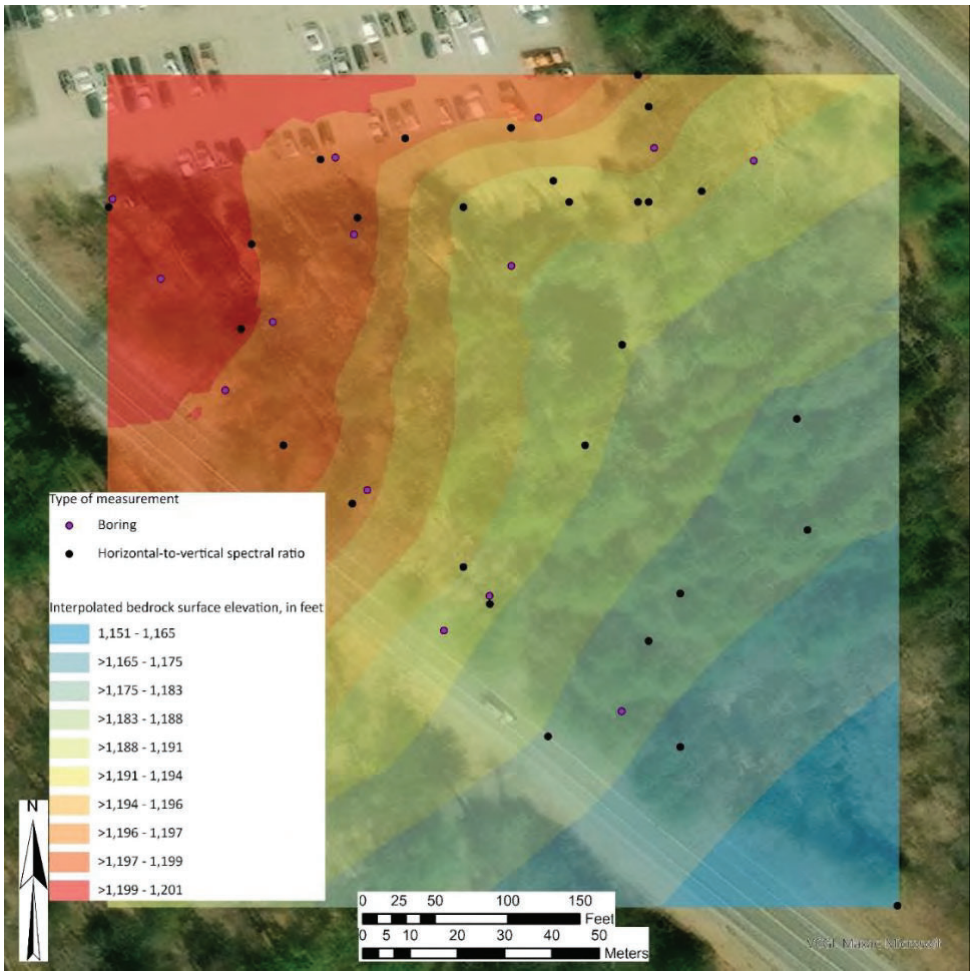

Figure 6. Map of the bedrock surface elevation calculated from passive seismic horizontal-to-vertical spectral ratio measurements at the carpool and bus stop parking site.

Bedrock outcropping was not observed at the site; therefore, shallow bedrock was not expected. However, this site had the most shallow bedrock of all the sites—as shallow as 5 ft in some locations (Table 1). The interpolated bedrock surface elevation map from HVSR results (fig. 6) indicates a higher elevation bedrock surface to the northwest that deepens to the southeast. Further, there is a northwest-southeast trending shallow trough in the bedrock surface at the northern edge of the map just to the south of the existing carpool and bus stop parking site

(fig. 6). The bedrock surface is deeper in the location of the trough that also corresponds with the location of seeps with iron fouling and with thicker variably saturated overburden, interpreted from the EMI results (fig. 7).

The multiple-frequency EMI instrument results are high quality (consistently positive and showing smooth, non-noisy variation in space) and suggest sensitivity to the upper layer of materials and the bedrock surface because the various depths of the inverted electrical conductivity values are above and below the contact. However, results do not indicate a strong ability to distinguish soil layers or bedrock in the areas most affected by roadway runoff, likely because of legacy deicing chemical contamination (fig. 7, high EC values). Comparison of electrical conductivity data to boring information indicated topsoil and outwash generally had low bulk electrical conductivity values, alluvium had moderate electrical conductivity values, and fill (from existing parking lot) had the highest electrical conductivity values. Inverted electrical conductivity values with depth do not consistently show ability to discern between different soil layers in the borings.

The multiple frequency EMI instrument data was likely influenced by vehicles and other infrastructure in the parking lot. Evidence of this influence was apparent based on large positive returns of in-phase components observed when surveying near the parking lot. Interference from metal items near the parking lot rendered EMI data uninterpretable and therefore could not be used to delineate the subsurface electrical conductivity in this area. The remainder of the site (forested area in fig. 7) exhibited low interference and yielded data free of noise contamination.

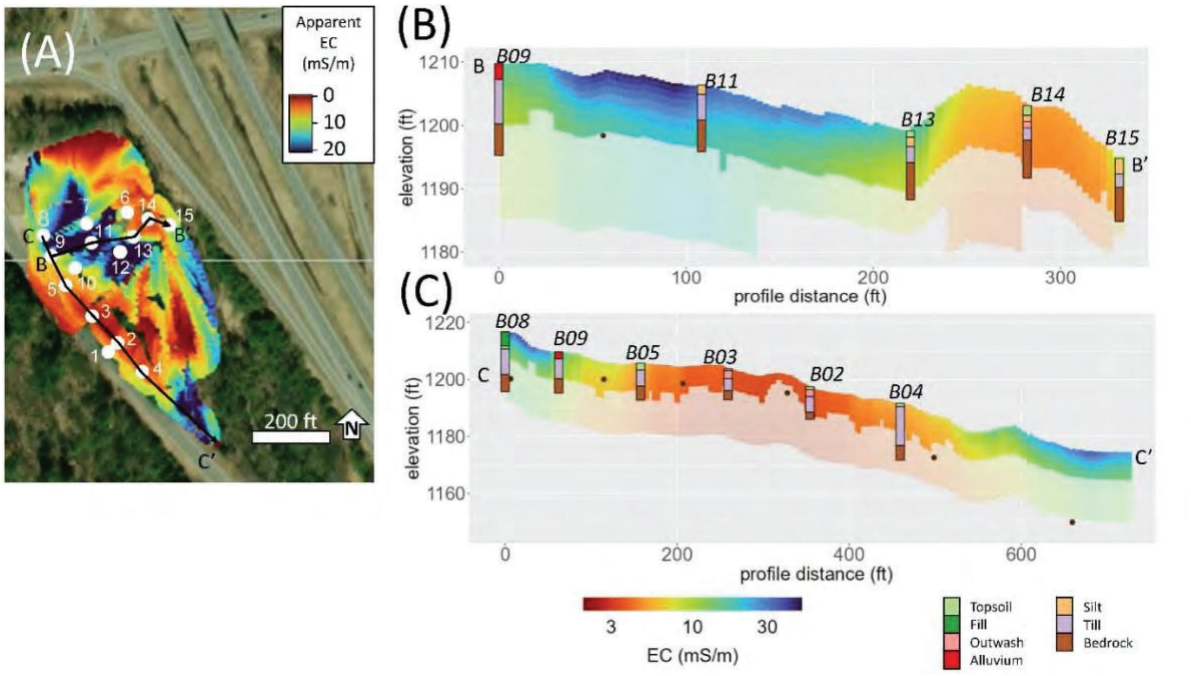

Figure 7. Electrical conductivity (EC) from electromagnetic induction survey results from the multiple-frequency instrument from the B-B' and C-C' cross sections at site 3, carpool and bus stop parking, New London, New Hampshire, showing (A) map of apparent electrical conductivity from the 47,970 Hz band and cross section locations. The white circles show boring locations. (B) and (C) show cross sections demarcated in (A) of inverted electrical conductivity with the bedrock surface from passive seismic horizontal-to-vertical spectral ratio results shown with black dots and borings identified.

Railroad adjacent to slope failure, site 4, Canterbury, New Hampshire

The railroad adjacent to slope failure site (site 4) is located in Canterbury, NH, on the east (left) bank of the Merrimack River to the west of Interstate Highway 93 (fig. 8b). The river reach has an oxbow meander bend with a cutbank that causes erosion and sediment transport, which also has caused failure in the slope above. The top of the slope failure scarp is approximately 20 ft from the railroad and 100 vertical feet above the riverbed. This site does not have an active geotechnical drilling investigation, but driller's logs are available from a previous hydrogeologic investigation associated with a formerly proposed landfill (Aries Engineering, Inc., 2005). The geophysical surveys at the site were scoped to determine the bedrock surface elevation and overburden stratigraphy at and adjacent to the slope failure.

Thirty-two HVSR measurements were made at locations along the top of the slope failure scarp, on the failed slope, and in a grid pattern in the adjacent wooded area between the railroad and Interstate 93. One of the HVSR locations was adjacent to a boring location with documented overburden stratigraphy and depth to bedrock, and the other 31 measurements were used to delineate the bedrock surface (fig. 8).

The multiple-coil-spacing EMI instrument was used to collect data along three survey lines at the railroad adjacent to the slope failure site. Apparent conductivity values were inverted and provided stratigraphic information to depths of 40 ft below land surface. Survey line 1 was parallel to the river and the closest survey line to the river. Electromagnetic induction results from survey line 1 showed an approximately 6 ft thick resistive layer overlying a conductive layer (fig. 9). Survey line 2 was upslope and parallel to the river (and line 1) and had an approximately 3-6 ft thick resistive layer overlying a conductive layer. At some locations along survey line 2 the conductive material was observed near the surface, which was corroborated by varved clay and silt seen in outcrop adjacent to the line. Survey line 3 was perpendicular to and south of survey lines 1 and 2. Low conductivity sand with minimal variation in EC values was indicated in results from survey line 3 (not shown), and inversion results had a very shallow depth of investigation, likely due to a low signal overall from resistive ground. In general, conductivity increased with distance from the river in lines 1 and 2.

Ground penetrating radar (GPR) was used only at this site, to improve the interpretation of the subsurface stratigraphy. Results provided information as deep as 100 ft in many locations. Penetration of the GPR signal was enhanced in electrically resistive materials and was best along lines 1 and 3 on the slope failure and above the scarp where the stratigraphy was relatively undisturbed by the failure.

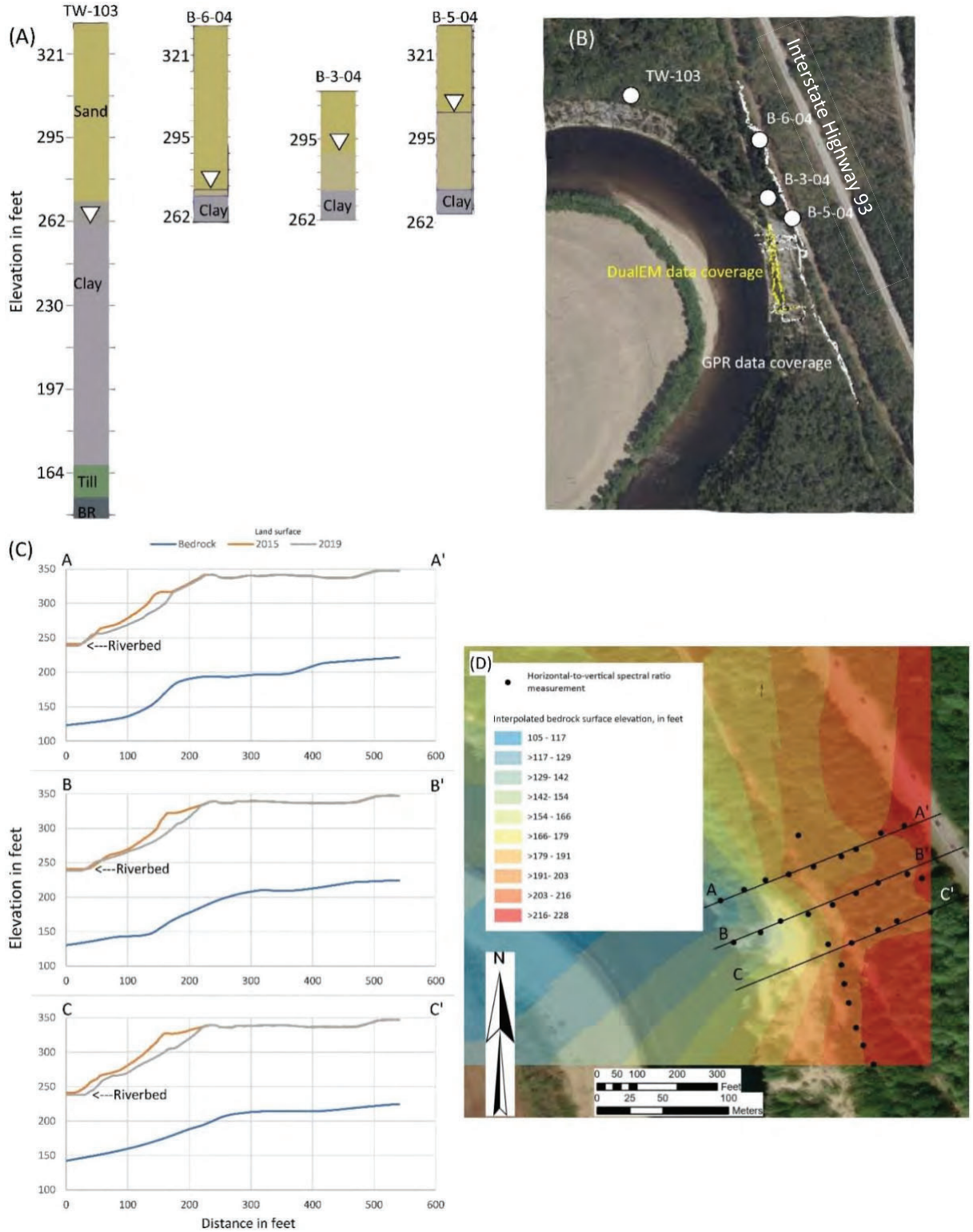

Figure 8. Boring logs and passive seismic horizontal-to-vertical spectral ratio measurement results from the A-A', B-B', and C-C' cross sections at site 4, railroad adjacent to slope failure, Canterbury, New Hampshire, showing (A) lithologic logs, (B) boring location map, (C) cross sections of the bedrock surface and land surface, and (D) map of interpolated bedrock surface elevation from passive seismic horizontal-to-vertical spectral ratio measurements.

The bedrock surface elevation delineated by HVSR is higher towards the northeast. The location of the bedrock surface does not provide any protection from additional riverbank erosion as it is well below (approximately 100 ft) the bed of the river (fig. 8B and C) and would not limit channel migration.

The B-B' EMI profile suggests conductive materials (fine sands or clays) below resistive materials (sands) (fig. 9B). The C-C' EMI profile suggests conductive materials (fine sands or clays) below resistive materials (sands), which are deeper compared to the B-B' line (fig. 10).

Ground penetrating radar data identified many anomalies that could not be interpreted because of limited information from wells and (or) test pits. Some layered GPR reflectors are indicated by the different colored arrows in fig. 11; these are likely soil layers or in the slope, possibly features related to the slope failure, such as fissures or shear planes (fig. 11B and C). The red arrows may indicate the water table in the C-C' GPR cross section (fig 11C) because the reflector is near the previously identified water-table depth (Aries Engineering, Inc., 2005).

The multiple-coil-spacing EMI instrument and GPR data are of high quality. Near-river profiles show a high resistivity layer over a high conductivity layer. A reasonably strong GPR reflector, that gets deeper closer to river, is also present.

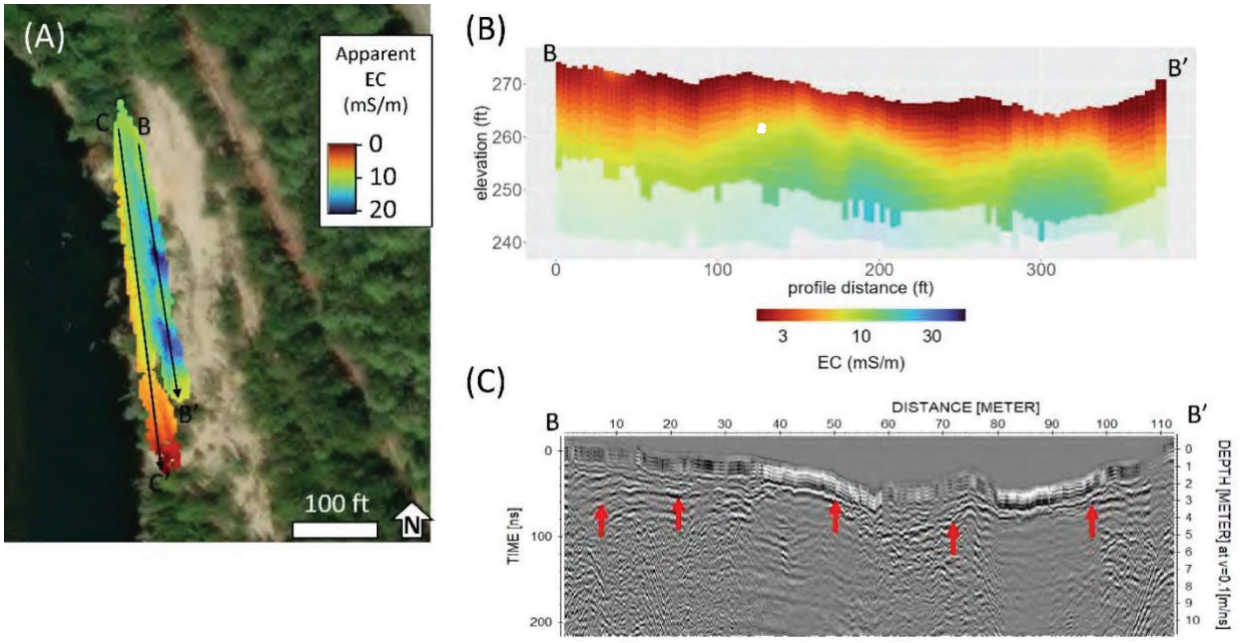

Figure 9. Multiple-frequency electromagnetic induction instrument and ground-penetrating radar survey results from the B-B' cross section at site 4, railroad adjacent to slope failure Canterbury, New Hampshire, showing (A) map of apparent electrical conductivity (EC) from the 4-m-spaced horizontal coplanar coils and cross section locations, (B) cross section of inverted electrical conductivity, and (C) ground-penetrating radar survey results.

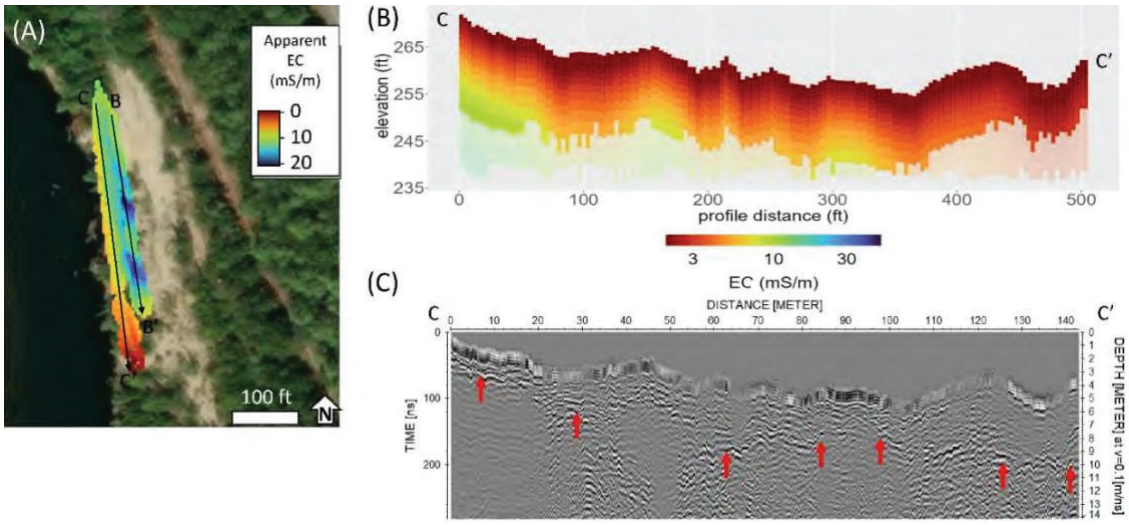

Figure 10. Multiple-frequency electromagnetic induction instrument and ground-penetrating radar survey results from the C-C' cross section at site 4, railroad adjacent to slope failure Canterbury, New Hampshire, showing (A) map of apparent electrical conductivity (EC) from the 4-m-spaced horizontal coplanar coils and cross section locations, (B) cross section of inverted electrical conductivity, and (C) ground-penetrating radar survey results.

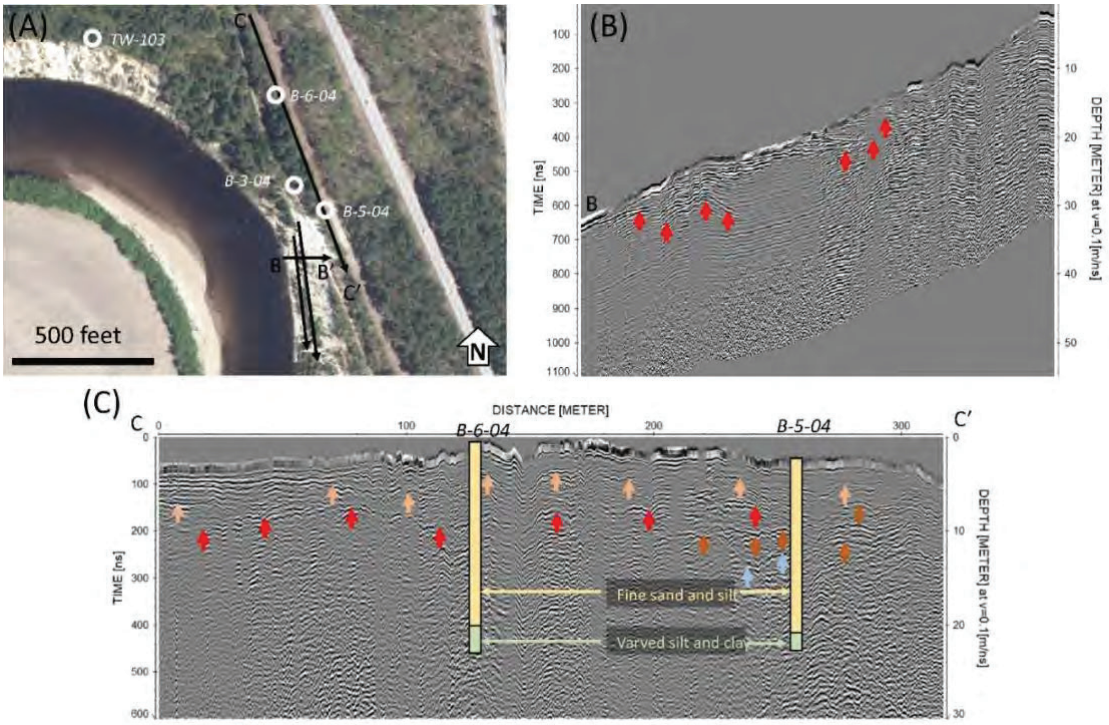

Figure 2. Ground penetrating radar results at site 4, railroad adjacent to slope failure Canterbury, New Hampshire, showing (A) map of survey and boring locations, (B) B-B' cross section, and (C) C-C' cross section. Different colored arrows indicate multiple reflectors that were observed. Materials described by boring logs and their depths are indicated along this profile.

SUMMARY AND CONCLUSIONS

The utility of geophysical techniques to supplement geotechnical investigations was evaluated during this study. Application of geophysical surveys using horizontal-to-vertical spectral-ratio (HVSR) passive-seismic and electromagnetic-induction (EMI) surveys near geotechnical borings at New Hampshire Department of Transportation (NHDOT) project sites showed that additional information on the bedrock surface could be provided beyond what was identified by borings alone. Results from HVSR and EMI surveys enhanced the information from existing borings and successfully delineated topographic highs and lows in the bedrock surface. At some sites, troughs in the bedrock surface were delineated, whereas at other sites bedrock highs, in the form of buried ridges or knobs, were detected. For example, at the roadway crossing rail trail site (site 1), higher elevation bedrock was discovered just south of the bridge. At this site, boreholes had a horizontal resolution of about 200 ft in the vicinity of the bridge and geophysical surveys expanded the extent by an order of magnitude with the same or better resolution along a 2,000-ft long survey line.

Information from geophysical surveys, when combined with geotechnical data from borings, can lead to more detailed interpretations by filling in data gaps between borings. Additionally, geophysical surveying is a cost-effective way to enhance drilling operations and can provide greater resolution or a larger extent at geotechnical investigation sites given the right conditions are met for each method. The instruments used were quick and easy to deploy, do not require permanent installation of equipment or excavation of material, and can be used in areas that are inaccessible to drill rigs. For example, borehole drilling was difficult in wooded areas at the carpool and bus stop parking site (site 3); however, it was possible to collect geophysical data in wooded areas. In addition, HVSR is passive, requiring no artificial sound source, as is required with traditional seismic refraction bedrock detection techniques. These additional data points helped identify a southeast sloping bedrock surface and trough beneath the forest that was only partially apparent from the borings.

Sediment EC variability was detected with EMI and when interpreted with HVSR, drillers' logs, or GPR can indicate general sediment grain size. For example, the fine grained varved sediment at the railroad adjacent to slope failure site (site 4) were further defined with GPR. This site also had the lowest mean electrical conductivity measured with the multiple-coil-spacing EMI instrument despite having the most conductive fine-grained material indicated in the lithologic logs. Electrical conductivity at the other sites may have been elevated due to buried metal, their proximity to areas affected by runoff with road salt applied for deicing, which likely increases the overall conductivity of sites near roadways. When dissolved in runoff, road salt can increase the specific conductance of water, which can contribute to increases in the apparent conductivity of vadose-zone infiltration and groundwater recharge that are detectible with EMI instruments.

Horizontal-to-vertical spectral ratio measurement results appeared to provide more definitive subsurface information than EMI methods at most sites because HVSR data were not sensitive to buried metal objects or too much of the above-ground infrastructure; however, the added value that EMI provides for identifying and delineating stratigraphy and characterizing different zones of groundwater quality make the combination of HVSR and EM useful. Additionally, the HVSR and EMI methods were able to successfully characterize the subsurface in most areas despite being near roadways with sources of interference such as vehicle traffic, electromagnetic noise (powerlines), and buried debris (bridge and railroad sites). Data collection

and analyses presented here have also furthered the understanding of how geophysical methods can help delineate features important to water availability, such as the bedrock surface, and to help identify zones with different groundwater quality. Future use of geophysical methods at NHDOT project sites have the potential to enhance the Department's site assessments in design and construction phases (Boeckmann and Loehr, 2016).

REFERENCES CITED

Abraham, Jared, Deszcz-Pan, Maria, Fitterman, David, and Burton, Bethany, 2006, Use of a handheld broadband FDEM induction system for deriving resistivity depth images, in Symposium on the Application of Geophysics to Engineering and Environmental Problems, 19, Las Vegas, Nevada, February 10–14, 2002, Proceedings: Denver, Colo., Environmental and Engineering Geophysical Society CD–ROM, p. 1782–1799.

Aries Engineering, Inc., 2005, Proposed Concord Regional Solid Waste/Resource Recovery Landfill Evaluation, Canterbury, New Hampshire, 42 pages

Beres, Milan, Jr., and Haeni, F.P., 1991, Application of ground-penetrating-radar methods in hydrogeologic studies: Ground Water, v. 29, no. 3, p. 375–386.

Bignardi, S., 2017, The uncertainty of estimating the thickness of soft sediments with the HVSR method: A computational point of view on weak lateral variations: Journal of Applied Geophysics, v. 145, p. 28-38., http://www.sciencedirect.com/science/article/pii/S0926985117302422

Boeckmann, Andrew Z. and Loehr, J. Erik, 2016, Influence of Geotechnical Investigation and Subsurface Conditions on Claims, Change Orders, and Overruns A Synthesis of Highway Practice, Transportation Research Board, National Academy of Sciences, 76 p., ISBN 978-0-309-27204-9, https://doi.org/10.17226/21926Carr, A. R., 2022a, Test Boring Report, Troy, 40371, State of New Hampshire Department of Transportation Materials & Research Bureau - Geotechnical Section, 23 pages

Carr, A. R., 2022b, Test Boring Report, New London 42877, State of New Hampshire Department of Transportation Materials & Research Bureau - Geotechnical Section, 15 pages

Christiansen, A. V. and Auken, E., 2012, A global measure of depth of investigation: Geophysics, v. 77, p. WB171-WB177.

Cox, B.R., Cheng, T., Vantassel, J.P., and Manuel, L., 2020, A statistical representation and frequency-domain window-rejection algorithm for single-station HVSR measurements: Geophysical Journal International, v. 221, no. 3, p. 2170-2183., https://doi.org/10.1093/gji/ggaa119

Degnan, J.R., Welch, S.M., White, E.A., Johnson, C.D., and Benthem, A.J., 2022, Passive seismic horizontal-to-vertical spectral ratio measurements at transportation infrastructure sites in New Hampshire, 2022: U.S. Geological Survey data release, https://doi.org/10.5066/P943EEFQ.

DUALEM-Manual, DUALEM website, accessed December 2022 at DUALEM.COM

Evenson, E.J., Orndorff, R.C., Blome, C.D., Bohlke, J.K., Herschberger, P.K., Langenheim, V.E., McCabe, G.J., Morlock,S.E., Reeves, H.W., Verdin, J.P., Weyers, H.S., and Wood, T.M., 2012, Strategic directions for U.S. Geological Survey water science, 2012–2022—Observing, understanding, predicting, and delivering water science to the Nation: U.S. Geological Survey Open-File Report 2012–1066, 42 p.

Fairchild, G.M., Lane, J.W., Jr., Voytek, E.B., and LeBlanc, D.R., 2013, Bedrock topography of western Cape Cod, Massachusetts, based on bedrock altitudes from geologic borings and

analysis of ambient seismic noise by the horizontal-to-vertical spectral-ratio method: U.S. Geological Survey Scientific Investigations Map 3233, 1 sheet, maps variously scaled, 17-p. pamphlet, on one CD–ROM. (Also available at http://pubs.usgs.gov/sim/3233.)

Geophex, Ltd. 2009, GEM-2 Broadband EMI sensor: accessed January, 2009 at http://www.geophex.com/GEM-2/GEM-2%20home.htm

Haeni, F.P., 1996, Use of ground-penetrating radar and continuous seismic-reflection profiling on surface-water bodies in environmental and engineering studies in Carpenter, Phil, ed., Groundwater Geophysics Special Issue: Journal of Environmental and Engineering Geophysics, v. 1, no. 1, p. 27–35.

Huang, Haoping, and Won, I.J., 2000, Conductivity and susceptibility mapping using broadband electromagnetic sensors: Journal of Environmental and Engineering Geophysics, v. 5, no. 4, p. 31–41.

Ibs-von Seht, M., Wohlenberg, J., 1999. Microtremor measurements used to map thickness of soft sediments. Bull. Seismol. Soc. Am. 89 (1), 250–259. http://refhub.elsevier.com/S0926-9851(17)30242-2/rf0090

Jacques Whitford Company, Inc., 2004, Construction Details of Wells and Piezometers Proposed Concord Cooperative Landfill Access Road, 17 pages

Johnson, C.D. and Lane, J.W., Jr., 2016, Statistical comparison of methods for estimating sediment thickness from horizontal-to-vertical spectral ratio (HVSR) seismic methods: An example from Tylerville, Connecticut, USA, in Symposium on the Application of Geophysics to Engineering and Environmental Problems, March 20-24, 2016, Denver, Colorado, 7 p., https://water.usgs.gov/ogw/bgas/publications/SAGEEP2016-Johnson/SAGEEP2016-Johnson.pdf

Johnson, C.D., White, E.A., Werkema, D., Terry, N., Phillips, S.N., Ford, R., and Lane, J.W., 2019, GEOPHYSICAL ASSESSMENT OF A PROPOSED LANDFILL SITE IN FREDERICKTOWN, MISSOURI: Symposium on the Application of Geophysics to Engineering and Environmental Problems 2019, https://doi.org/10.4133/sageep.32-031.

Kearey, P., and Brooks, M., 1991, An introduction to geophysical exploration second edition: Blackwell Scientific Publications, Cambridge, Mass., 254p

Lane J. W. Jr, White, E. A., Steele, G. V., & Cannia, J. C. (2008). Estimation of bedrock depth using the horizontal-to-vertical (H/V) ambient-noise seismic method. In: Symposium on the Application of Geophysics to Engineering and Environmental Problems, Philadelphia, Pennsylvania, Proceedings: Denver, Colorado, Environmental and Engineering Geophysical Society, p. 13, 6–10 Apr 2008.

Mack T.J. (2020) Passive Seismic Survey of Sediment Thickness, Dasht-e-Nawar Basin, Eastern Afghanistan. In: Guth P. (eds) Military Geoscience. Advances in Military Geosciences. Springer, Cham., https://doi.org/10.1007/978-3-030-32173-4_12

Marvinney, R.G. and Glover, H., 2015, The influence of the Presumpscot Formation on seismic hazard in southern coastal Maine, 2015 Symposium on the Presumpscot Formation, Portland, ME, 20 p.

Medler, C.J., 2022, Delineating the Pierre Shale from geophysical surveys east and southeast of Ellsworth Air Force Base, South Dakota, 2021: U.S. Geological Survey Scientific Investigations Map 3497, 3 sheets, 15-p. pamphlet, https://doi.org/ 10.3133/ sim3497.

Milsom, J. and Eriksen, A. (2011). Ground Penetrating Radar. In Field Geophysics (eds J. Milsom and A. Eriksen). https://doi.org/10.1002/9780470972311.ch10

MOHO, 2020, Tromino Blu Portable ultra-light acquisition system for seismic noise and vibrations, International patents: Pub. No. WO2006011021 (A1), Pri. No. IT2004BO00449 20040719, USPTO 7.800.981, USER'S MANUAL, 144 p.

Nakamura, Y., 1989. A method for dynamic characteristics estimation of subsurface using microtremor on the ground surface. Quarterly Report of Railway Technical Research Institute 30, 25–33. http://refhub.elsevier.com/S0926-9851(17)30242-2/rf0125

Nakamura, Y., 2000. Clear identification of fundamental idea of Nakamura's technique and its applications. Proceedings of the 12th World Conference on Earthquake Engineering (8 pp., New Zealand). http://refhub.elsevier.com/S0926-9851(17)30242-2/rf0130

Jeeban Panthi, Carole D. Johnson, Soni M. Pradhanang, Brian Savage, Mamoon Y. Ismail, Thomas B. Boving, 2023, Delineating bedrock topography with geophysical techniques: An implication for groundwater mapping, CATENA, Volume 230, 107258, ISSN 0341-8162, https://doi.org/10.1016/j.catena.2023.107258.

R Core Team, 2023, R: A language and environment for statistical computing. R Foundation for Statistical Computing, Vienna, Austria. URL https://www.R-project.org/.

U.S. Department of Transportation, Federal Highway Administration, 2020, Advanced Geotechnical Methods in Exploration (A-GaME), Center for Accelerating Innovation web page, accessed 03/31/2021, https://www.fhwa.dot.gov/innovation/everydaycounts/edc_5/geotech_methods.cfm

SESAME WP04, 2004. Guidelines for the implementation of the H/V spectral ratio technique on ambient vibrations measurements, processing and interpretation.

Welch, S.M., Degnan, J.R., and Terry, N.C., 2023, Electromagnetic induction and ground-penetrating radar surveys at transportation infrastructure sites in New Hampshire, 2022: U.S Geological Survey data release.

Wickham, H., 2016, ggplot2: Elegant Graphics for Data Analysis. Springer-Verlag New York, ISBN 978-3-319-24277-4, https://ggplot2.tidyverse.org.

Yuengling, K. R., 2022, Test Boring Report, Lee, 41322, State of New Hampshire Department of Transportation Materials & Research Bureau - Geotechnical Section, 8 pages

Zohdy, A.A.R., Eaton, G.P., and Mabey, D.R., 1974, Application of surface geophysics to ground-water investigations: U.S. Geological Survey Techniques of Water-Resources Investigations, book 2, chap. D1, 86 p., http://pubs.usgs.gov/twri/twri2-d1/